Available at www.scientevents.com/proscience/

ScientEvents

ProScience 3 (2016) 21-30

Conference Proceedings

2nd International Conference on Atmospheric Dust - DUST2016

Estimates of ground surface characteristics for outbreaks of the Asian Dust Storms in the sources region

Yuta Demura[1], Buho Hoshino[2*] Yuki Sofue[1*], Kenji Kai[3], Ts. Purevsuren[1], Kenji Baba[2], Jun Noda[4]

[1]Graduate School of Dairy Science, Rakuno Gakuen University, Japan
[2]College of Agriculture, Food and Environment Sciences, Rakuno Gakuen University, Hokkaido, Japan
[3]Graduate School of Environmental Studies, Nagoya University, Japan
[4]Department of Veterinary Science, Rakuno Gakuen University, Japan
[*]aosier@rakuno.ac.jp

Abstract

The Inland Asian dry land, such as Gobi and desert of Mongolian Plateau is the most important dust source region in the world. However, in recent years the dust storms were found to have out-broken from the pastureland around the dry lakes, dry river channels and degraded pasturelands. Surrounding of dry lake beds, dry river channels and degraded pastures are the main new sources of Asian Dust Storms (ADS). In this study, based on satellite data, we measured of the Critical Ground Surface Condition (CGSC) (such as vegetation index (NDVI), soil moisture index (SMI), terrain roughness index (TRI), and soil particles) in ASD source region, to establish their influence on ADS and evaluate the mechanism of their occurrence.

Keywords: Asian dust emissions; The critical ground surface condition; Ground surface characteristics; Remote sensing

1. Introduction

The Inland Asian dry land, including Mongolian Gobi and desert area is the most important dust source region in the world. The major driving forces for land degradation and desertification include global climate change (nature dynamics) and anthropogenic changes (human dynamics) (e.g., Cochrane et al., 2009; IPCC, 2014). The climate change

ISSN: 2283-5954
Selection and peer-review under responsibility of DUST2016 Scientific Committee
DOI:10.14644/dust.2016.004

in this area is responsible for poor vegetation. In response to the climate change and anthropogenic changes, the source area of Asian Dust Storm (ADS) is located up north with respect to the Inner Mongolian degraded pastureland and Mongolian drought water bodies, and away from the traditional ADS source area associated with Taklimakan desert and Loess Plateau (Demura et al., 2015). Main environmental factors that affect ASDs occurrences, their intensity, and heights are (i) atmospheric stability (a low pressure, ascending current); (ii) wind speed (strong westerlies); and (iii) source region surface characteristics. Other additional factors: (iv) surface heating; (v) soil moisture content; (vi) soil type; and (vii) surface vegetation (roughness). Moreover, strong surface heating can provide the necessary buoyancy to elevate dust to great heights. Dust storm frequency and intensity vary largely from one location and event to another.

Inland dry lake beds (DLBs) and dry river channels have become a new source of ADS (Batima et al., 2005; Natsagdorj et al., 2001; Demura et al., 2015). The dust storm outbreak in springtime is affected mainly by a strong wind and particular ground surface conditions such as type of vegetation, the presence of dead grass remaining, bare land, snow cover, and/or types of dust particles. These conditions are not mutually exclusive; thus, it is complicated to understand the process of dust storm outbreak in Mongolian Gobi and desert.

This study focuses on the ground surface conditions to analysis the dead grass coverage, soil moisture and dry lake beds surfaces that may affect the dust storm outbreak. Among the three surface types, the dry lake beds are considered to contribute a substantial amount of global dust emissions and to be responsible for "hot spots" of the dust outbreaks. However, the significance of dry lake beds to total dust storm outbreaks has not been clarified in Mongolian Gobi and desert area. Furthermore, it has been suggested that the dead grass may have decreased in dust storm outbreak in the Mongolian grassland. The dead grass attributes as surface roughness elements which affect dust particles transport and dust storm outbreaks. However, the effect of the dead grass on desert surface to restrict dust storm outbreaks has not been clarified in the Mongolian Gobi and desert.

2. Materials and methods

2.1 Estimate of the hot-spot of the Asian Dust Source emission

Qu et al. (2006) developed a "dust index", Normalized Dust Difference Index (NDDI), and a categorization methodology, the Asian dust categorization. The NDDI can be written as follows (1).

$$NDDI = \left(\rho_{2.13\mu m} - \rho_{0.469\mu m}\right)/\left(\rho_{2.13\mu m} + \rho_{0.469\mu m}\right) \quad (1)$$

where $\rho_{2.13\mu m}$ and $\rho_{0.469\mu m}$ are reflectance at the top of atmosphere (TOA) in the 2.13 and 0.469 μm wavelengths respectively. This study used the TOA reflectance of MODIS band 3 (0.459-0.479 μm), and band 7 (0.2105-0.2155 μm), respectively. MODIS-Terra products (MOD021KM) were used to evaluate the ADS area on May 11, 2011. The dust index and categorization methodology shows blowing dust intensity and accurately identifies dust, clouds and ground surface. The Asian dust categorization is performed with brightness temperature (BT) difference and NDDI. We succeeded in identification of the ground surface, dust and a cloud in the Gobi and desert region based on NDDI and BT difference using MODIS data (Fig. 1).

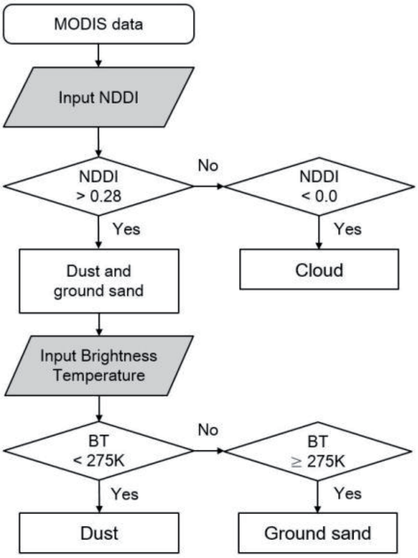

Fig. 1. The flow chart of the algorithm for extracting NDDI from MODIS data

In the case study, the data set was obtained for a particular dust event (on May 11, 2011, GMT 13:13:42) over South Eastern Gobi and desert region of Mongolia. We identified distribution areas of different concentration levels of the dust using the method reported in Fig. 1 and information from Fig. 2. In this dust event wind directions, based on European Centre for Medium-range Weather Forecasts (ECMWF), were the northwest and north-northwest and the wind velocity reached 17-18 m/s on May 11, 2011. The analysed area was classified to three buffer zones from the dust storm spot in the direction of the windward (Fig. 3). The dry lake beds (DLBs) became the hotspots of the Asian dust outbreak.

The NDDI values in the DLBs are higher than in other areas. Since the surface soil of the DLBs is carried from highlands to lowlands by fluvial processes (e.g., river networks in Fig. 3) during the warm period and the DLBs dries up significantly in the dry season, there is a large quantity of clay (particles < 0.004 mm) deposits on the DLBs surface (Shao, 2008).

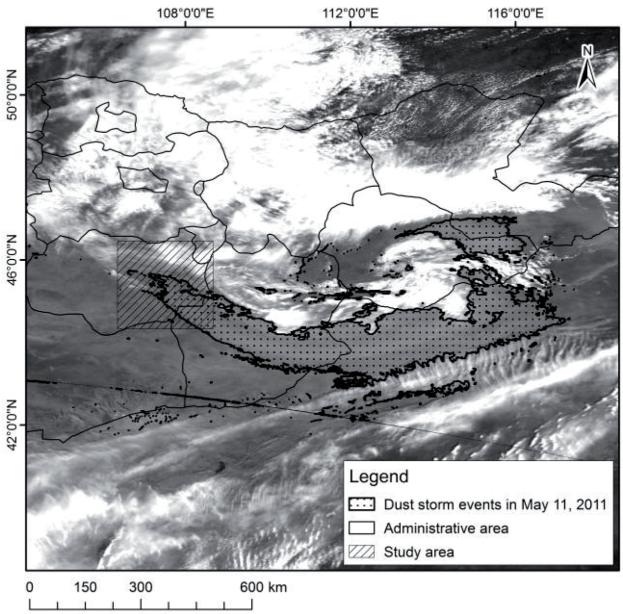

Fig. 2. The dust event over the Gobi and Desert analyzed using NDDI

2.2 Ground Measurement of Spectral Characteristic

Field measurements of the ground spectral characteristic were performed in April 27 to 29, 2015. The ground measurements, including Photosynthetic vegetation (PV), Non-photosynthetic vegetation (NPV) and Bare land (BL), were obtained using ASD FieldSpec spectroradiometer for three dates (Fig. 4). The values of the ground spectral measurement for NIR and Red reflectance were aggregated into a mean reflectance for each of the same wavebands of Terra MODIS in order to compare the differences between the BL and the NPV of NDVI. We used linear discriminant analysis to discriminate between two naturally occurring groups. The discriminant analysis was used to determine which continuous variables can discriminate between two or more naturally occurring groups (i.e., BL and NPV).

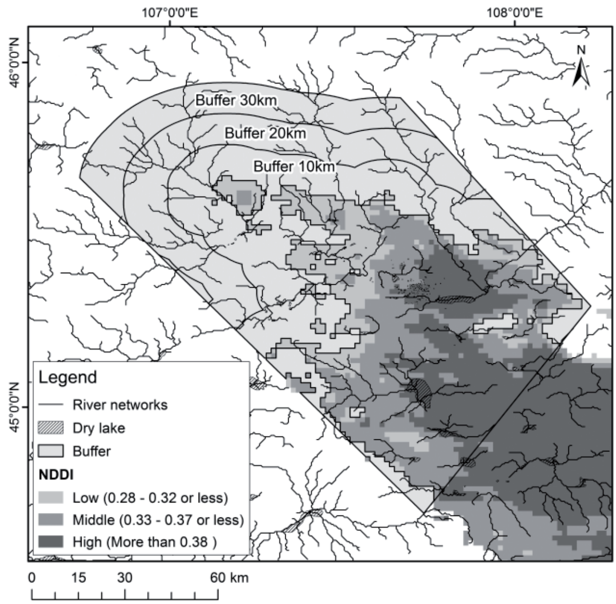

Fig. 3. 30 km buffer zone in the direction of the windward from the spot where sand whirled up

2.3 *Critical Ground surface Condition and Statistical Comparative Method*

The Normalized Difference Vegetation Index (NDVI) is a numerical indicator that uses the visible red and near-infrared bands of electromagnetic spectrum to analyse EM, signatures of live green vegetation by remote sensing. The NDVI can be written as in the equation (2) (Tucker, 1979):

$$NDVI = (NIR - Red) / (NIR + Red) \quad (2)$$

where, Red and NIR stand for the spectral reflectance measurements acquired in the visible red and near-infrared regions, respectively. MODIS-Terra eight-day 250 meter atmospheric-corrected reflectance products (MOD09Q1) were used to evaluate the land cover conditions from May 11 to 16, 2011.

The soil moisture model of radiative transfer from the earth's surface must incorporate the effects of the observable such as temperature brightness. Soil Moisture Index (SMI) based on an empirical parameterization of the relationship between surface temperature (Ts) and NDVI (Wang et al., 2009), the SMI can be written as the in the equation (3).

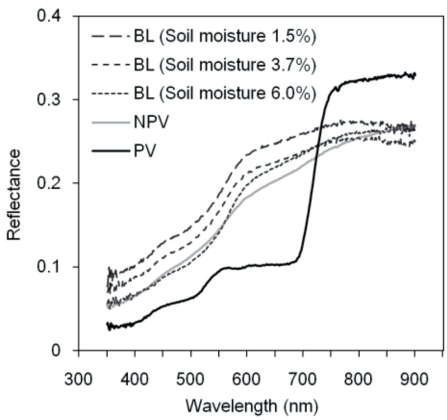

Fig. 4. Spectral characteristic of the ASD ground spectral measurements in the study area

$$SMI = (LST_{max} - LST) / (LST_{max} - LST_{min}) \quad (3)$$

where LST_{max} and LST_{min} are, respectively, the maximum and minimum land surface temperature value for a given NDVI; and LST is the remotely sensed data derived land surface temperature at a given pixel for a given NDVI. MODIS-Terra MOD09A1 and MOD11A1 products were used to evaluate the NDVI and Ts from May 11 to 16, 2011. The Terrain Roughness Index (TRI) was calculated from 90-m spatial resolution Shuttle Radar Topography Mission (SRTM) in combination with the digital elevation model (DEM) data using a terrain analysis function implemented in a geographic information system (GIS). If each square represents a GIS grid cell on a DEM, then TRI can be calculated by using the equation (4) (Riley, et al., 1999).

$$TRI = Y \left\{ \sum (X_{ij} - X_{00})^2 \right\}^{1/2} \quad (4)$$

where, X_{ij} is elevation of each neighbour cell (i, j) to cell (0, 0).

The soil particle data used digital soil map from the International Soil Science Society (ISSS) and SoilGrids1km (Hengl et al., 2014). Data set is expressed as concentration of clay (%) in the surface soil data.

2.4 Potential Lake and Dry Lake Beds (DLBs) Detection Method Based on Feature Extraction in Remote Sensing Images

The Normalized Difference Water Index (NDWI) was used to quantify the detected surface waters in wetland environments and to allow for the measurement of surface water extent (Gao, 1996). The NDWI can be written as (equation (5)):

$$\text{NDWI} = (\text{Red} - \text{SIR}) / (\text{Red} + \text{SIR}) \quad (5)$$

where, Red is the TOA red reflectance and SIR is the TOA short-wave infrared reflectance. Ji et al. (2009) asserted that values of NDWI greater than zero are assumed to represent water surfaces, while values less than, or equal, to zero are assumed to be non-water surfaces.

This paper presented potential lake and dry lake detection method based on feature extraction in remote sensing images. The method separated the potential lake regions from the images by extracting multiple dimensional feature parameters to describe the different properties of the wet and dry areas and other areas.

Firstly, using the NDWI images obtained in July, August and September from 2000 to 2014 the method extracts the pixel-based maximum NDWI (pixels corresponding to the wettest area). The NDWI is greater than zero. Secondly, NDWI image is masked by SRTM DEM data with the slope of less than 2 degrees. Finally, this method can give the index of wet or dry areas in the images of the potential lake area by quoting the values of the NDWI. This can be performed on the annual basis. The workflow of the method is illustrated in Fig. 5.

2.5 Analysis of Trends and Breakpoints in the Critical Ground Surface Condition

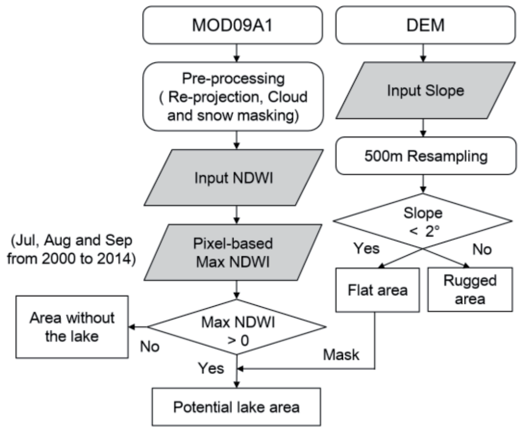

Fig. 5. The flowchart of the detection method for potential late area based on feature extraction in remote sensing images

Analysis of past years of DLBs, wind velocity and NDVI data may reveal that ADS are changed gradually over the period of time. In statistics and probability theory, a point process is a type of random process for which any one realisation consists of a set of isolated points either in time or geographical space or in even more general spaces. With this in mind, NDVI and wind velocity can be considered normal time series data, but the DLBs is a point process data.

NDVI and wind velocity time series data typically contain trend, remainder and seasonal component. We investigate the application of a generic change detection method that accounts for seasonality and enables the detection of trend change within the time series (Verbesselt et al., 2010). The key concepts of this method for detecting Breaks For Additive Seasonal and Trend (BFAST) is an iterative algorithm that combines the decomposition of time series into seasonal, trend, and remainder component with methods for detecting changes. The methods are available in the BFAST package for R (R Development Core Team, 2011) from CRAN (http://cran.r-project.org/package=bfast). An additive decomposition model is used to iteratively fit a piecewise linear trend and a seasonal model. The general model is of the form (equation (6)):

$$Y_t = T_t + S_t + e_t \quad : t \in T \tag{6}$$

where, at time t (in the time series T), Y_t is the observed NDVI and wind velocity value, T_t is the trend component, St the seasonal component en et the remainder component which contains the variation beyond what is explained by T_t and S_t.

This study examined this effect using detection of trend changes in NDVI satellite data between 2000 and 2014. Time series of 690 weekly images were analysed using a trend breaks analysis (BFAST) procedure. And NDVI satellite data was analysed by a simple method based on the Savitzky-Golay filter (Savitzky, et al., 1964) to more efficiently reduce contamination in the NDVI time series that is caused primarily by cloud contamination and atmospheric variability.

The DLBs data set was constructed from a set of isolated points either in time or geographical space, or in even more general spaces. The DLBs and lake in the potential lake area are affected by precipitation variation. It is necessary that this influence is quantitatively evaluated to discover new source areas of the Asian dust outbreaks. We use Welch's t-test (Welch, 1947) which is well-suited for this case as the number of samples for each random variable is different and relatively large. This analysis can be written as (equation (7)):

$$t = \left(\overline{X}_1 - \overline{X}_2\right) / \sqrt{\frac{s_1^2}{N_1} + \frac{s_2^2}{N_2}} \tag{7}$$

where, $\overline{X}_1$, s_1^2 and N_1 are the first sample mean, sample variance and sample size, respectively. This paper compares precipitation in dry lake seasons and precipitation in lake seasons. In this study, precipitation data was used Global Precipitation Climatology Project (GPCP), which was added up to the precipitation of every eight days to compare it with the period of MODIS 8-days composite images.

3. Result and discussions

3.1 Result of Dry Lake beds (DLBs) detection Using Remote Sensing Images

As a result of having classified DLBs and areas without lake by detection method based on feature extraction in remote sensing image, the DLBs was extracted in study area which was bigger than 500 m resolution (Fig. 6). However, when the area of DLBs is smaller than MODIS 500 m spatial resolution, the area of DLBs cannot be extracted under the influence of spatial resolution (Fig. 6c-d). The problems of the spatial resolution and mixed pixels are considered as due to these influences. The importance and impact of spatial resolution is also documented by the mixed pixel problem. Mixed pixels sometimes occur where the image pixels are not homogenous, or pure. Instead a pixel contains a measure of the energy reflected or emitted from several different materials or land surface objects and the sensor records a composite of these responses. Even if these problems are considered, the experimental results indicate that the proposed method is capable of effective discrimination between DLBs area and areas without lake.

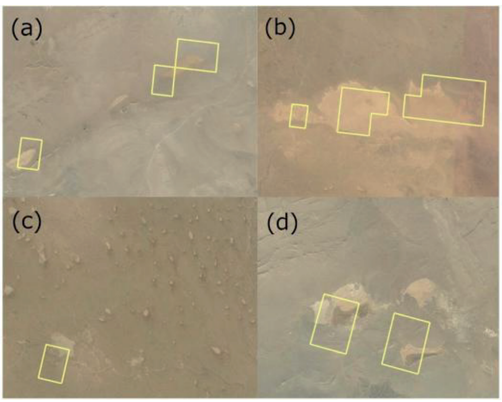

Fig. 6. Dry lake Beds (DLBs) detection result of same images in study area. The yellow square area is the area extracted by potential lake and dry lake detection method

3.2 Characterization of the Ground Spectral Measurement

The ground spectral measurements including Photosynthetic Vegetation (PV), Non-Photosynthetic Vegetation (NPV) and Bare Land (BL) were obtained from 38 sites in study area (Demura et al., 2015).

As it can be seen from Fig. 7, the boundary (NDVI = 0.1) can be used to distinguish the BL from the NPV according to the result of the discriminant analysis. The classification accuracy was found to be with 100% (BL) and 71% (NPV). In light of these spectral characteristics it can be easily concluded that BL and NPV have 0.1 of the linear threshold.

3.3 Critical Ground Surface Condition for Asian Dust Storm Outbreak

Statistical comparative result for the Critical Ground Surface Condition (CGSC) such as NDVI, Soil particles (clay), SMI and TRI in the Asian dust storm sources area, with the influence on dust storm outbreak shows in Fig. 8. It shows two different areas of dust outbreak spots and buffer zones of the windward areas. As a result of having examined homogeneity of variance by Bartlett's test (Kruskal et al., 1952), the variances in the groups are not the same ($p>0.001$). Thus using the Steel-Dwass official approval of the multiple comparison method, a comparison of results showed: (1) with NDVI and TRI, significant differences were confirmed between all groups ($p<0.001$). This means flat terrain (plain) vegetation shows low NDVI value; (2) Shows in Fig. 8, with Soil Particles, without a group between "Buffer 10 km" area to "HighNDDI" area; and "LowNDDI" area to "MiddleNDDI" area, and other testing showed all having statistical significance. With "LowNDDI" area to "HighNDDI" area ($p<0.01$) and "MiddleNDDI" area to "HighNDDI" area ($p<0.05$), and others area showed $p<0.001$ (see Fig. 8). The concentration of clay is high in the Buffer 30 km area and "HighNDDI" area. This result suggests that Soil Particles are carried from highlands to lowlands by river networks; (3) with the SMI, "Buffer 30 km" area to "Buffer 20 km" area do not differ significantly and others area are significantly different ($p<0.001$). The SMI is relatively higher in dust outbreak spot than in the buffer area because of the influence of the DLBs formed of the catchment topography.

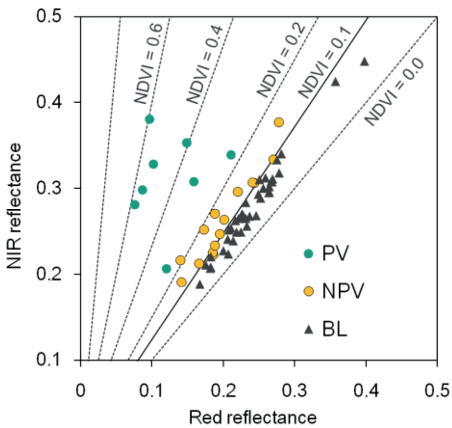

Fig. 7. Ground spectral measurement for each NIR and Red waveband of Terra MODIS. A solid line (NDVI = 0.1) is the linear boundary between BL and NPV from the result of the linear discriminant analysis

In dust storm seasonal events, spring NDVI is generally low value in comparison with other seasons (e.g., summer and autumn). In addition, the planimetric feature of study area like Mongolian Gobi and desert region is distributed of BL, a small amount of PV and NPV. NPV of NDVI is low value than PV of NDVI (e.g., 0.1-0.2) and BL of NDVI is low value than NPV of NDVI (e.g., 0.1 or less) in Fig. 7. NDVI data shown in Fig. 8 (a) that groups which were smaller than the threshold at 0.10 was BL. "Buffer 20 km" area to "Buffer 10 km" area and "LowNDDI" area to "MediumNDDI" area were less than the threshold. NDVI value of "LowNDDI" area was the lowest in all groups, which was the median of 0.085 (see Fig. 8). As a result, we can argue that decrease in NDVI affects the dust storm outbreak.

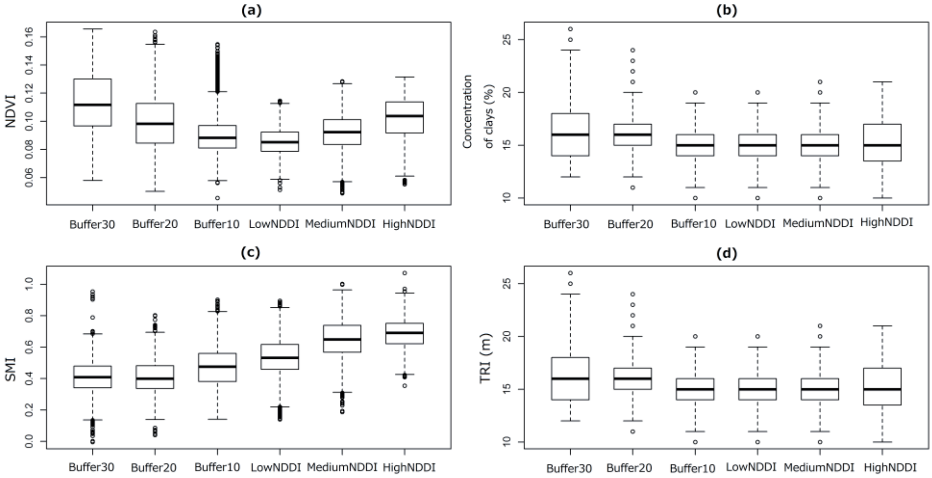

Fig. 8. Statistical test results between (a) NDVI and NDDI; (b) soil particles (soil clay (%) and NDDI; (c) SMI and NDDI and (d) TRI and NDDI in dust outbreak spots and its buffer areas. Low NDDI, Medium NDDI and High NDDI is located in dust outbreak spots

4. Concluding remarks

In this study we confirmed that there is a high correlation between outbreaks of the Asian dust and the ground surface characteristics of sources region.

In the field survey, we measured a reflectance of bare land, a dry grass (NPV) and green grass (PV) and clarified a difference of the distribution of these feature in the R-NIR spectrum feature space.

The potential lake and dry lake beds (DLBs) detection method results indicate that the proposed method is capable of reasonable discrimination between DLBs area and areas without lakes effectively. We also indicated that the increase of the number of DLBs was affected by a decrease in precipitation.

Statistical test results for the Critical Ground Surface Condition (CGSC) such as NDVI, Soil particles (concentration of clay (%) in surface soil), SMI and TRI in the Asian dust storm sources area, including the influence on dust storm outbreaks, show that the Asian dust storms that occurred in the past originated from the dry basins, where hot spots of vegetation were poor and where many lakes had dried up. We inferred that the dried-up lake in the Inland Asia was a new source of outbreaks of the Asian Dust Storms.

Of particular importance for ADS outbreaks, as discovered in this work, is high wind speed. Finally, we suggest that the DLBs, NDVI and TRI of spatial dispersion influence the border between outbreak and non-outbreak on the ground surfaces.

5. Acknowledgements

This work was supported by Grant-in-Aid for Scientific Research (A) (No.) 16H02703 (2016-2021), Grant-in-Aid for Challenging Exploratory Research (No.) 25550079 (2013-2016) and Grant-in-Aid for Scientific Research (B) (No.) 24340111 (2013-2015) from

JSPS of Ministry of Education, Culture, Sports, Science and Technology and Scientific Joint Research Project of Rakuno Gakuen University (2014-2016).

References

Batima P., Natsagdorj L., Gombluudev P., Erdenetseteg B. (2005). Observed climate change in Mongolia. AIACC Working Paper 12, 12-16.

Cochrane K., Young C.D., Soto D., Bahri T. (2009). *Climate change implications for fisheries and aquaculture: overview of current scientific knowledge*. Food and Agriculture Organization of the United Nations (FAO) 530, 1-203.

Demura Y., Hoshino B., Sofue Y., Kai K., Purevsuren Ts., Baba K., Chen J., Mori K. (2015). Estimates of critical ground surface condition for Asian dust storm outbreak in Gobi desert region based on remotely sensed data. IEEE IGARSS 2015(1), 870-873. DOI: http://dx.doi.org/10.1109/IGARSS.2015.7325903.

Gao B. (1996). NDWI – A normalized difference water index for remote sensing of vegetation liquid water from space," Remote Sensing of Environment 58, 257-266.

Hengl T., de Jesus J.M., MacMillan R.A., Batjes N.H., Heuvelink G.B.M., Ribeiro E., Samuel-Rosa A., Kempen B., Leenaars J.G.B., Walsh M.G., Gonzalez M.R. (2014). SoilGrids1km - Global Soil Information Based on Automated Mapping. PLoS ONE 9(12), 1-16.

Hollander M., Wolfe D.A. (1999). *Nonparametric Statistical Methods* (Second Edition). New York: John Wiley and Sons. pp 213-315.

IPCC (2014). In: Climate Change 2014: Impacts, Adaptation, and Vulnerability. *Part A: Global and Sectoral Aspects. Contribution of Working Group II to the Fifth Assessment Report of the Intergovernmental Panel on Climate Change*. Field, C.B., V.R. Barros, et al., (eds.). pp 1-32.

Ji L., Zhang L., Wylie B. (2009). Analysis of dynamic thresholds for the normalized difference water index," Photogrammetric Engineering and Remote Sensing 75, 1307-1317.

Kruskal W.H., Wallis W.A. (1952). Use of ranks in one-criterion variance analysis," Journal of the American Statistical Association 47, 583-621.

Natsagdorj L., Dulamsuren J. (2001). Some aspects of assessment of the dzud phenomena. Papers in Meteorology and Hydrology 23, 3-8.

Qu J.J., Hao X., Kafatos M., Wang L. (2006). Asian Dust Storm Monitoring Combining Terra and Aqua MODIS SRB Measurements. IEEE Geoscience and Remote Sensing Letter 3, 484-486.

Riley S.J., DeGloria S.D., Elliot R. (1999). A Terrain Ruggedness Index That Quantifies Topographic Heterogeneity," Intermountain Journal of Science 5, 23-27.

Savitzky A., Golay M.J.E. (1964). Smoothing and differentiation of data by simplified least squares procedures," Journal of Analytical Chemistry 36, 1627-1639.

Shao Y. (2008). *Physics and Modelling of Wind Erosion (second edition)*," Springer. pp 91-115.

Tucker C.J. (1979). Red and photographic infrared linear combinations for monitoring vegetation. Remote Sensing of Environment 8, 127-150.

Verbesselt J., Hyndman R., Newnham G., Culvenor D. (2010). Detecting trend and seasonal changes in satellite image time series. Remote Sensing of Environment 114, 106-115.

Wang L., Qu J.J. (2009). Satellite remote sensing applications for surface soil moisture monitoring: A review," *Frontiers of Earth Science in China* 3(2), 237-247.

Welch B.L. (1947). The Generalization of `Student's' Problem when Several Different Population Variances are Involved. Biometrika 34, 28-35.